CrossMark

Wetting and Interfacial Chemistry of Sn-Zn-Ga Alloys with Cu Substrate

Tomasz Gancarz and Przemyslaw Fima

Wetting of Cu pads by Sn-Zn eutectic-based alloys with 0.1, 0.2, 0.5, and 1.0 wt.% of Ga was studied using the sessile drop method in the presence of ALU33® flux. Wetting tests were performed at 250 °C after 60, 180, 480, 900, 1800, and 3600 s of contact, and at 230, 280, 320 °C for a contact time of 480 s. After cleaning the flux residue from solidified samples, the spreadability of Sn-Zn-Ga on Cu was determined in accordance with ISO 9455-10:2013-03. Selected, solidified solder-pad couples were cross-sectioned and subjected to scanning electron microscopy with energy dispersive spectroscopy and x-ray diffraction study of the interfacial microstructure. Growth of the intermetallic Cu_5Zn_8 and $CuZn_4$ phase layers was studied at the solder-pad interface. Samples after spreading test at 250 °C for 60 s were subjected to aging for 1, 10, and 30 days at 170 °C.

1. Introduction

Sn-Zn-based alloys are a group of alloys of particular interest as Pb-free solders in the electronics industry. It has been reported that alloying elements such as Ag, Al, Bi, Cu, etc. were added to Sn-Zn eutectic (Sn-Zn$_{eut}$) to improve its wetting, mechanical properties, and corrosion resistance (Ref 1, 2). The Ga element, unlike many others, does not form intermetallic compounds (IMCs) with Sn and Zn, and exhibits a relatively broad range of solid solubility in both Sn and Zn (Ref 3, 4). Song et al. (Ref 5), Hung et al. (Ref 6), and recently Gancarz (Ref 7) studied the effect of Ga concentration (up to 1.8, 0.8, and 3.0 wt.%, respectively) on the microstructure of cast alloys. They observed coarsening of Zn-rich precipitates and increasing size of the Sn-phase, as Ga content increased. Due to its low melting temperature (29.8 °C), even small additions of Ga to Sn-Zn eutectic decreases the melting temperature, yet, the solidus decreases faster than the liquidus, resulting in broadening of the pasty range (Ref 5, 8). Although Zhang et al. (Ref 8) were the first to present a ternary Sn-Zn-Ga phase diagram obtained by piecing binary phase diagrams, Zivkovic et al. (Ref 9) used the Calphad approach and thermodynamic descriptions of binary systems only, for that purpose. They found the calculated pseudo-binary (Sn-Zn$_{eut}$)-Ga diagram to be in agreement with transition temperatures determined with differential thermal analysis (DTA). Their calculations indicate that

the solubility limit of Ga in solid Sn-Zn$_{eut}$ is about 5 at.%, and that the Ga-rich liquid phase exists at room temperature above this threshold (Ref 9).

The increase of tensile strength of Sn-Zn-xGa alloys with Ga content, accompanied by decrease of elongation as observed in Ref 5-7, is caused by the solid solubility of Ga in Sn and Zn. Hung et al. (Ref 6), with the use of secondary ion mass spectrometry (SIMS), compared the thickness of the oxide film on the surface of as-cast Sn-9Zn and Sn-9Zn-0.4Ga (wt.%) and found it to be 50% thinner in the latter case. Based on this, and on the thermal behavior of oxide film on Sn-9Zn-0.4Ga (wt.%), they assumed that Ga increases oxidation resistance. The effect of Ga content (up to 3 wt.%) on wetting on the Cu substrate, for 30 s, at 235 °C, and on the thickness of the IMC interlayer formed, was studied only by Chen et al. (Ref 10). More recently, Ye et al. (Ref 11) characterized the microstructure of the interface between the Sn-9Zn-0.5Ga alloy and the Cu substrate after a wetting balance test at 235 °C and subsequent aging for 100 h at 100 °C. In this study, we investigated the effect of temperature and extended time of contact on the spreading areas of Sn-8.9Zn-xGa alloys (x = 0.1, 0.2, 0.5, 1.0 wt.%) on the Cu substrate, and on the interfacial microstructure of Sn-8.9Zn-xGa/Cu joints. Selected joints were subjected to isothermal aging at 170 °C and the evolution of the interface was studied.

2. Experimental

Sn-8.9Zn-xGa solder alloys (x = 0.1, 0.2, 0.5, 1.0 wt.%) were prepared by melting precise amounts of high purity components: Sn, Zn, Ga (99.999 wt.%). To avoid oxidation, alloys were melted in graphite crucibles, in a resistance-heated furnace placed in a glovebox filled with high purity Ar (6N). For spreading tests, the as-cast solders were cut into pieces of ∼0.2 g each and degreased with acetone. Except for degreasing, there was no special treatment of the Cu (99.9 wt.%) substrates ($25 \times 20 \times 0.2$ mm). The tests were carried out with the setup earlier used in studies of Sn-Zn-X alloys (Ref 12), which enables the quick transfer of the sample to the already

Tomasz Gancarz and **Przemyslaw Fima,** Institute of Metallurgy and Materials Science, Polish Academy of Sciences, 30-059 Krakow, Poland. Contact e-mail: p.fima@imim.pl.

heated furnace, and out of it after the designated time of the test, so both the heating rate and cooling rate are high. To study the effect of extended time of contact and temperature on the evolution of the solder-substrate interface, samples were held at 250 °C for 60, 180, 480, 900, 1800, and 3600 s, and for 480 s at 230, 280, and 320 °C.

Wetting tests were performed with ALU33® flux (~0.05 cm^3) applied to the solder sample and surrounding part of the substrate. According to ISO 9454-1, this is 2.1.2-type flux, organic, water-soluble, and activated with halides. Its components are aminoethylethanolamine ($C_4H_{12}N_2O$) and ammonium fluoroborate (NH_4BF_4). The reported spreading areas are the average of three measurements on independent solidified samples after washing flux residue with tap water. After wetting tests, selected solidified solder/substrate couples were cut perpendicular to the plane of the interface, mounted in conductive resin and polished for microstructural characterization. Selected samples, after spreading test for 60 s at 250 °C, were subjected to aging at 170 °C for 24, 240, and 720 h. The microstructural and energy dispersive spectroscopy (EDS) analysis were performed using the Quanta 3D FEG system, at 20 kV, with the standardless Analysis EDAX System based on Genesis 4000 software.

3. Results and Discussion

3.1 Solder-Substrate Interaction

The spreading areas of Sn-8.9Zn-xGa alloys on Cu substrate after wetting at 250 °C for the designated time are presented in Fig. 1(a). With increasing time of contact, spreading areas of solders do not increase. On the contrary, the highest average value of the spreading area is observed after 60 s. In particular, for alloys containing 0.1 and 0.2 wt.% Ga, the spreading area is about the same, whereas for alloys containing 0.5 and 1.0 wt.% Ga, there is a tendency for the spreading area to decrease

as time of contact increases. The spreading area of the Sn-8.9Zn-1.0Ga alloy after 1800 s is 30% lower than for the same alloy after 60 s. Considering that the estimated error of the determined spreading area is up to 5%, this is not a big difference. Figure 1(b) illustrates the spreading area determined after 480 s at the designated temperature. One can see that, at 250, 280, and 320 °C, the spreading area is about 40 mm^2, whereas at 230 °C, the spreading area shows a decreasing tendency with increased Ga content, although the effect is not so clear considering the error bars. The average value of the spreading area is smaller than ~50 mm^2 reported for Sn-9Zn-xGa ($x = 0.1 \div 3$ wt.%) alloys (Ref 10). Chen et al. (Ref 10) showed that the spreading area, determined at 235 °C for solder samples of 0.2 g, increases with increasing Ga content, and above 0.5 wt.% Ga stabilizes at a constant level. When comparing the results of spreading area, it is important to remember that the spreading areas reported in Ref 10 were determined after 30 s, while the results presented in this paper (Fig. 1b) were determined after 480 s. While the main reason for this discrepancy is likely to be different flux, the type of flux and its activity was not specified in Ref 10.

The microstructures of Sn-Zn$_{eut}$ alloys with 0.5 wt.% Ga on Cu substrates after spreading at 250 °C for a contact time of: (a) 60; (b) 180; (c) 480; (d) 900; (e) 1800; (f) 3600 s, are presented in Fig. 2. For alloys containing 0.1, 0.2, and 1.0 wt.% Ga, the interfacial microstructure looks similar, with intermediate layers at the interface composed of IMCs from the Cu-Zn system. The curves labeled SnL (red), CuK (green), ZnK (dark blue), GaK (light blue) represent EDS line scan results along the bright line perpendicular to the plane of interface. Starting from the Cu substrate, concentration of Cu decreases from 100 to ~35 wt.% in Cu_5Zn_8, ~20 wt.% in $CuZn_4$, and 0 in Sn-8.9Zn-xGa alloy. One can see that concentrations of Ga and Sn in the intermediate layers are close to zero. After 60 s of contact time, an interlayer (~1 μm) is observed, which is composed of Cu_5Zn_8 and $CuZn_4$. On the other hand, Chen et al. (Ref 10) reported that only a Cu_5Zn_8 IMC layer is formed at the interface, after 30 s at 235 °C, followed by slow cooling in the furnace. Ye et al. (Ref 11) showed an optical micrograph of the
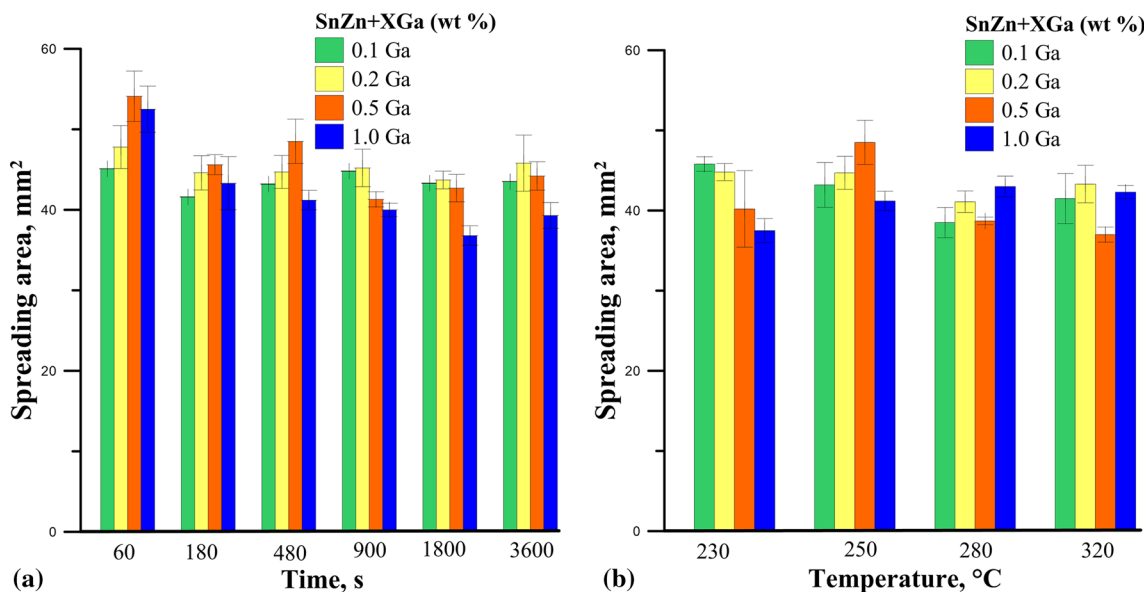

Fig. 1 Spreading area of Sn-8.9Zn-xGa alloys on Cu: (a) effect of time of contact, (b) effect of temperature
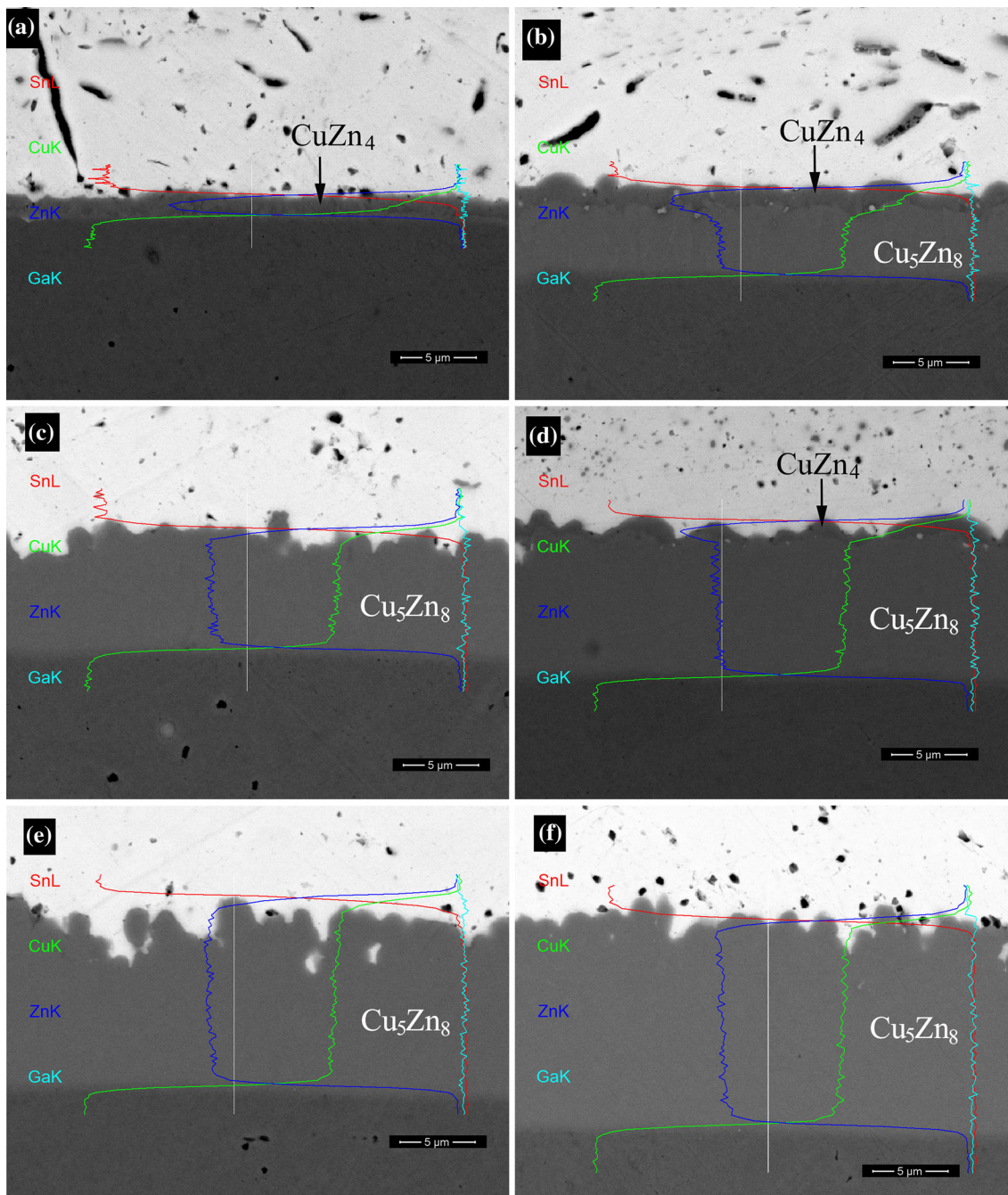
Fig. 2 Interfacial microstructure of Sn-8.9Zn-0.5Ga/Cu couples at 250 °C after the designated time of contact: (a) 60 s, (b) 180 s, (c) 480 s, (d) 900 s, (e) 1800 s, (f) 3600 s

Sn-9Zn-0.5Ga/Cu interface after a wetting balance test (immersion time 10 s), where, of the two interlayers, only the thicker one from the side of substrate was labeled as Cu_5Zn_8. After 180 s (Fig. 2c) both sub-layers can be easily distinguished. These are Cu_5Zn_8 from the side of the substrate, and a thinner $CuZn_4$ sublayer from the side of the solder. After 480 s the Cu_5Zn_8 is thicker, but $CuZn_4$ appears thinner, and spots of discontinuity can be observed. With increasing contact time the Cu_5Zn_8 continues to grow, but no $CuZn_4$ remains. The obtained microstructure of Sn-8.9Zn-xGa on the Cu substrate is similar to the Sn-Zn-In/Cu interface (Ref 13). However, the $CuZn_4$ layer is still present at the Sn-Zn-In/Cu interface after a long contact time (3600 s), as

opposed to the Sn-8.9Zn-xGa/Cu interface. The microstructures of the Sn-Zn-xCu/Cu (Ref 12) (time of contact up to 180 s) and Cu/Sn-Zn-Ag-Cu/Cu (Ref 14) joints differ from those of Sn-8.9Zn-xGa/Cu, because the IMCs from Cu-Zn to Ag-Zn systems are present in the solder. However, the microstructure of the Sn-Zn-Ag-Cu/Cu interface for a long contact time (1800 and 3600 s) is similar to that of Sn-8.9Zn-xGa/Cu, with only one Cu_5Zn_8 layer observed at the interface.

Considering solubility of Ga in Sn and Zn (Ref 3, 4) it can be assumed that interfacial microstructures of Sn-8.9Zn-xGa/Cu couples may be similar to Sn-9Zn/Cu couples and may similarly evolve in time. Although literature agrees that
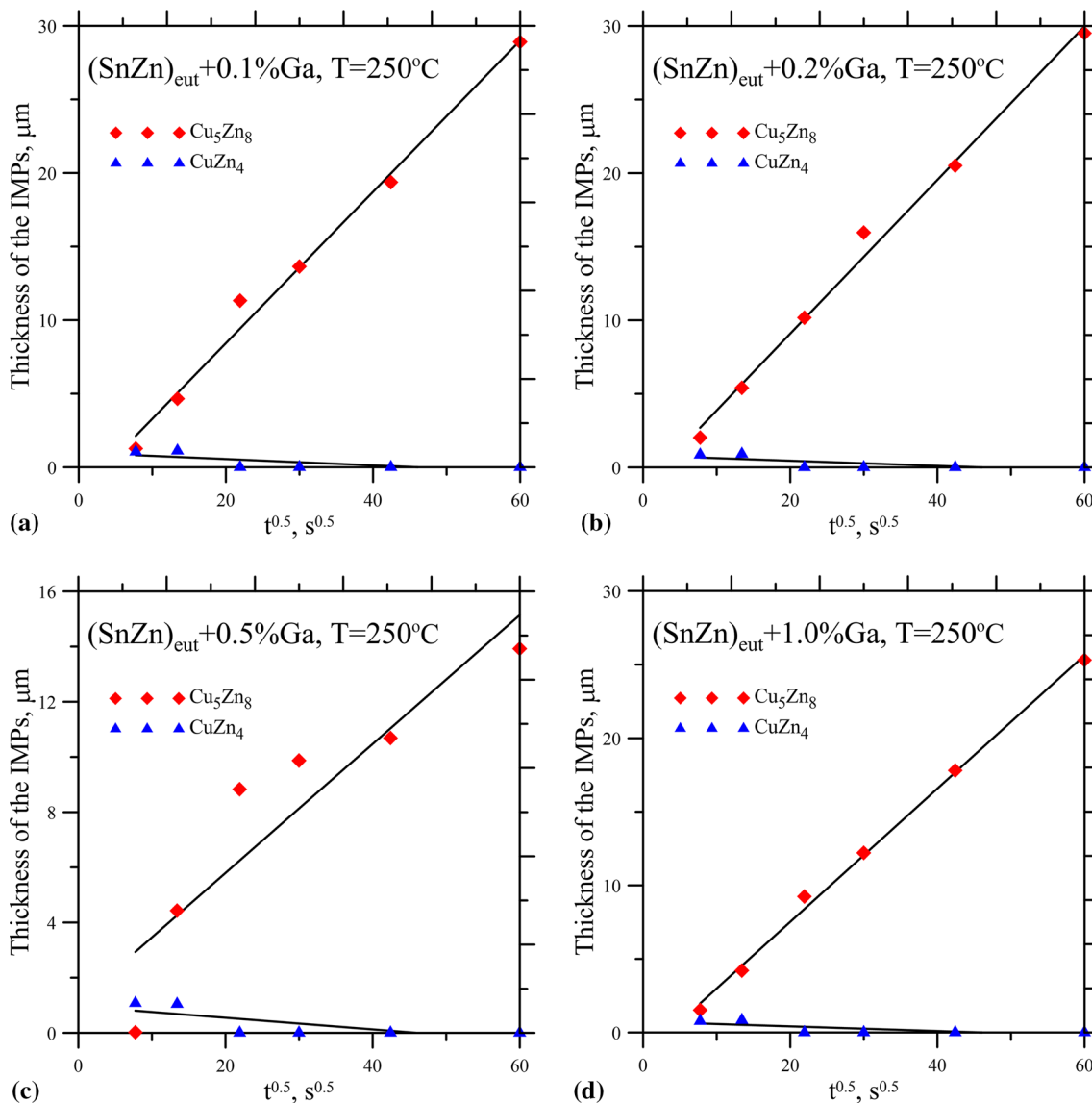
Fig. 3 Thickness of IMC layer at 250 °C for Sn-8.9Zn-xGa/Cu couples, where x equals: (a) 0.1, (b) 0.2, (c) 0.5, (d) 1.0 wt.%

thickness of Cu_5Zn_8 increases in time, there is some disagreement regarding $CuZn_4$. Lee and Shieu (Ref 15) reported for Sn-9Zn/Cu couples that $CuZn_4$ still exists after 480 s at 250 and 270 °C, and its thickness is greater than after shorter wetting time. Mayappan (Ref 16), on the other hand, found both $CuZn_4$ and $Cu5Zn_8$ after 60 s but only Cu_5Zn_8 layer after 180 s at 290 °C. Gibbs free energy of ε-$CuZn_4$ phase is less negative (higher) than that of β-Cu_5Zn_8 phase (Ref 17), meaning that the latter is thermodynamically more stable. This explains why Cu_5Zn_8 prevails over long time but does not explain why initially (at the beginning of wetting) there is also $CuZn_4$ present. Using a kinetic model with thermodynamic data Terashima and Sasaki (Ref 18) predicted that for Sn-xZn/Cu couples where $x < 10$ wt.%, the Cu_5Zn_8 is the only phase that is formed, which contradicts earlier studies (Ref 15, 16). As we have recently shown for Sn-8.9Zn-xCu/Cu couples (Ref 12), it seems that $CuZn_4$ is formed first because initially the influx of Zn towards Cu surface is greater than dissolution of Cu, so each Cu atom can bond with four Zn atoms. Once there is thin layer of $CuZn_4$, the Zn diffuses through it and reacts with Cu to form

Cu_5Zn_8, which growths continuously. Further existence of $CuZn_4$ depends on the influx of Zn from alloy to the interface.

The thickness of the IMC layer vs time is presented in Fig. 3, for different Ga content: (a) 0.1, (b) 0.2, (c) 0.5, and (d) 1.0 (wt.%). As the thickness of the Cu_5Zn_8 layer increases, the thickness of the $CuZn_4$ layer decreases. The thickness of Cu_5Zn_8 varies linearly with the square root of time, which is typical for diffusion-controlled growth (Ref 15). This can be expressed as $x = (k \times t)^{0.5}$, where: x is the thickness of the interlayer, k is the growth constant, and t is time. Growth and disappearing mechanism of $CuZn_4$ is obviously different, nevertheless we show the data for $CuZn_4$ in Fig. 3 for comparison purposes (the lines showing the decreasing tendency of $CuZn_4$ serve as a guide for an eye only, as we did not determine the k values for $CuZn_4$). We found that, at 250 °C, k for Cu_5Zn_8 equals 0.51 for 0.1 wt.% Ga, 0.52 for 0.2 wt.% Ga, and 0.45 for 1.0 wt.% Ga. For 0.5 wt.% Ga it is lower (0.23). The growth constant k of Cu_5Zn_8 is lower for Sn-8.9Zn-0.5Ga/Cu because, for a long contact time (1800 and 3600 s), the thickness of Cu_5Zn_8 is in this case lower than for the remaining
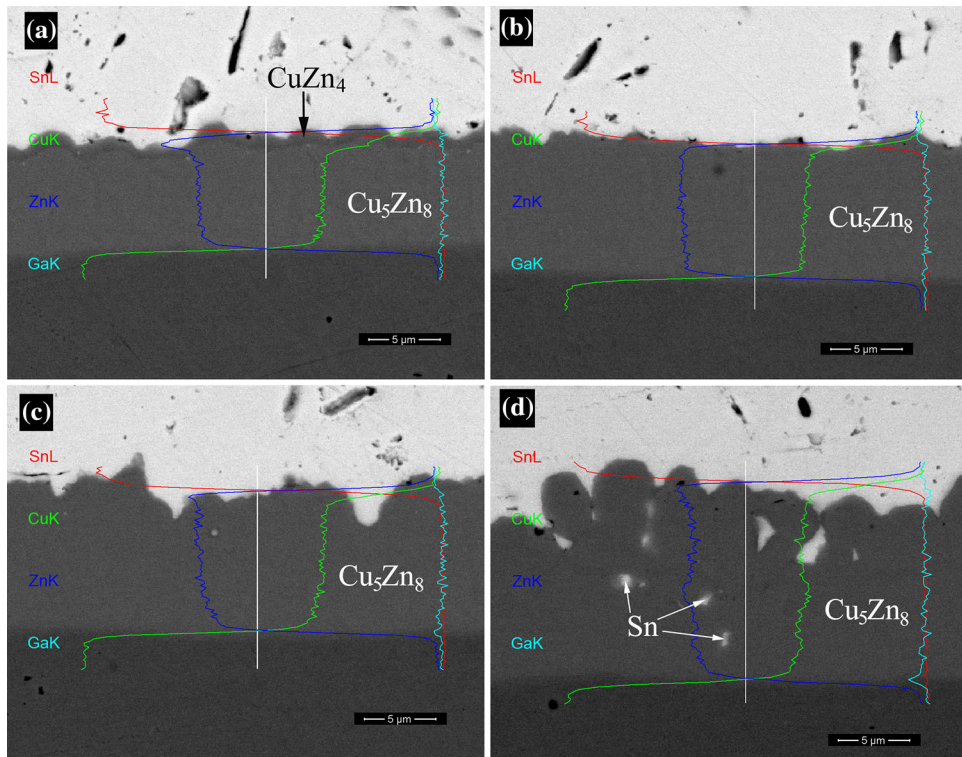
Fig. 4 Interfacial microstructure of Sn-8.9Zn-1.0Ga/Cu couples after 480 s at: (a) 230 °C, (b) 250 °C, (c) 280 °C, (d) 320 °C
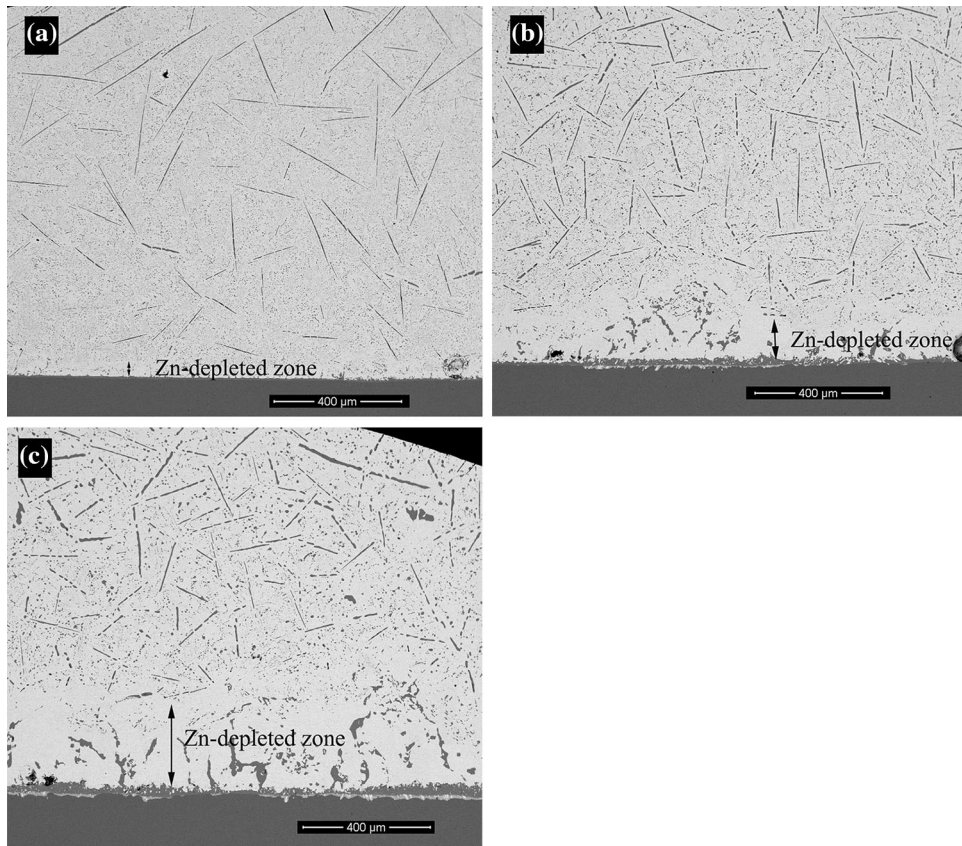

Fig. 5 Zn-depleted zone in Sn-8.9Zn-0.5Ga/Cu couples after spreading at 250 °C for 60 s, and subsequent aging at 170 °C for: (a) 24 h, (b) 240 h, (c) 720 h

interfaces. For short time of contact, the thickness of Cu_5Zn_8 is very similar for different Ga content and equals: 1.48 ± 0.41 μm at 60 s, 4.67 ± 0.52 μm at 180 s, and 9.89 ± 1.11 μm at 480 s. The fact that the thickness of the Cu_5Zn_8 IMC does not vary with different Ga concentrations for a short time of contact contradicts the earlier findings of Chen (Ref 10). According to Chen (Ref 10), the thickness of Cu_5Zn_8 increases with increased Ga content. Moreover, despite the lower temperature and short contact time (235 °C and 30 s) (Ref 10) the thickness of Cu_5Zn_8 layer in the case of 0.5 wt.% Ga alloy is 6 times greater than in present work. This difference, however, can be explained by different cooling regimes. In this study, the samples were transferred rapidly from the furnace to room temperature after the designated time. The samples of Chen et al. (Ref 10), however, were cooled slowly in the furnace, which kept the Cu_5Zn_8 growing. Slow cooling of samples might also explain why Chen et al. (Ref 10) did not observe the $CuZn_4$ phase. A different character of IMC growth was observed for Sn-Zn-In/Cu (Ref 13). In this case, despite dissolution of In in eutectic Sn-Zn, the $CuZn_4$ layer continued to grow over time. For Sn-Zn-Cu/Cu couples over a short time (60 s) (Ref 12), the IMC layer at the interface is twice as thick as the Sn-Zn-Ga/Cu IMC layer, despite the formation of Cu-Zn phases in Sn-Zn-Cu solder. This was different for Cu/Sn-Zn-Ag-Cu/Cu (Ref 14) with a long contact time (3600 s). In this case, the Cu_5Zn_8 phase has a similar thickness to that of Sn-Zn-0.5Ga/Cu, despite the addition of Ag and Cu, which creates an IMC layer at the interface, all other phases disappear over time, and only the Cu_5Zn_8 layer remains.

The microstructures of Sn-8.9Zn alloys with 1.0 wt.% Ga on Cu substrates after spreading test for 480 s at: 230, 250, 280, and 320 °C, are presented in Fig. 4. The thickness of the Cu_5Zn_8 layer increases with temperature, and the $CuZn_4$ layer is only observed at 230 °C. At 320 °C, Sn inclusions start to appear in the Cu_5Zn_8 layer (Fig. 4d). As a result, the Cu_5Zn_8 layer looks scalloped from the solder side. The scalloped structure and Sn inclusion are caused by higher diffusion of Cu to the solder at 320 °C. This results in the creation of a high Cu diffusion path in the Cu_5Zn_8 layer. A similar effect on the growth of the Cu_5Zn_8 layer was observed for Sn-Zn-Ag-Cu/Cu (Ref 14), where the addition of Ag and Cu formed $AgZn_3$ and $CuZn_4$ layers. However, with increasing time, these layers are dissolved.

3.2 Aging of Joints

After wetting for 60 s at 250 °C, cross-sectioned samples were subjected to aging treatment. The Sn-8.9Zn-0.5Ga/Cu couples, after aging at 170 °C for 24, 240, and 720 h, are presented in Fig. 5. With increasing aging time the intermetallic layer at the Sn-8.9Zn-0.5Ga/Cu interface gets thicker, but after 10 days the IMC layer becomes discontinuous. Zinc precipitates start to disappear in the solder close to the interface, and the size of zinc-depleted zone grows over time, as shown in Fig. 5. Large, irregular precipitates of Cu_5Zn_8 are formed in the solder close to the interface, because diffusion of Cu is much higher than that of Zn (Ref 19). The thickness of the IMC layer increases from the solder side due to the Cu subsequently
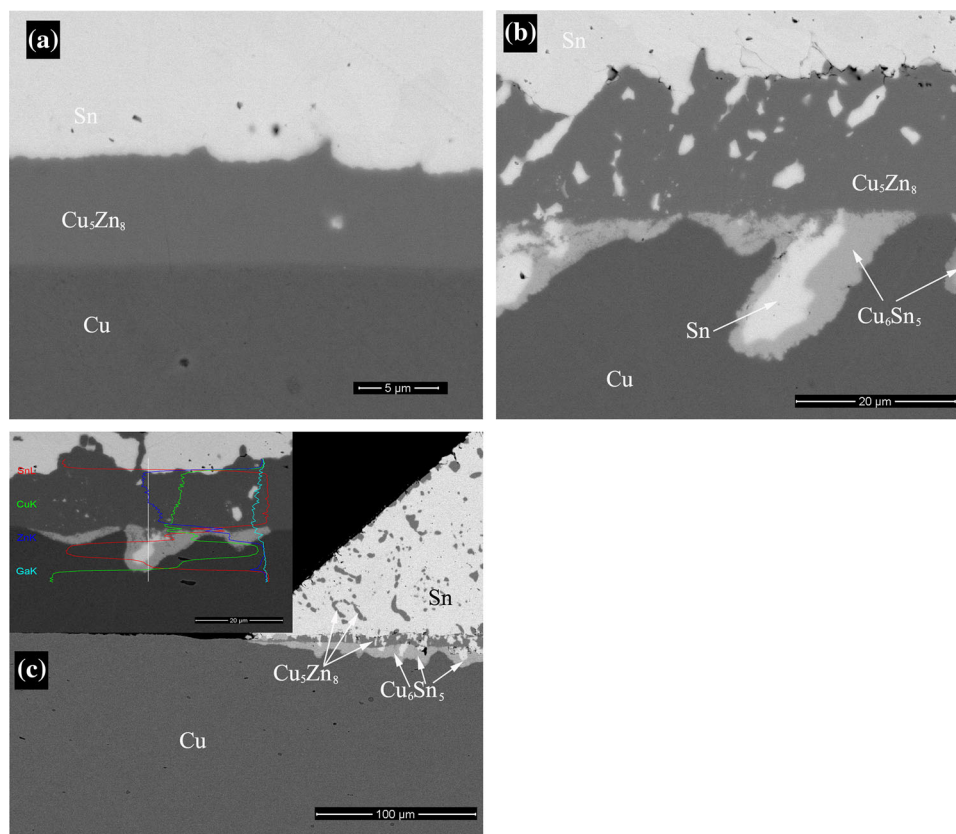

Fig. 6 Interfacial microstructure of Sn-8.9Zn-0.5Ga/Cu after spreading at 250 °C for 60 s, and subsequent aging at 170 °C for: (a) 24 h, (b) 240 h, (c) 720 h
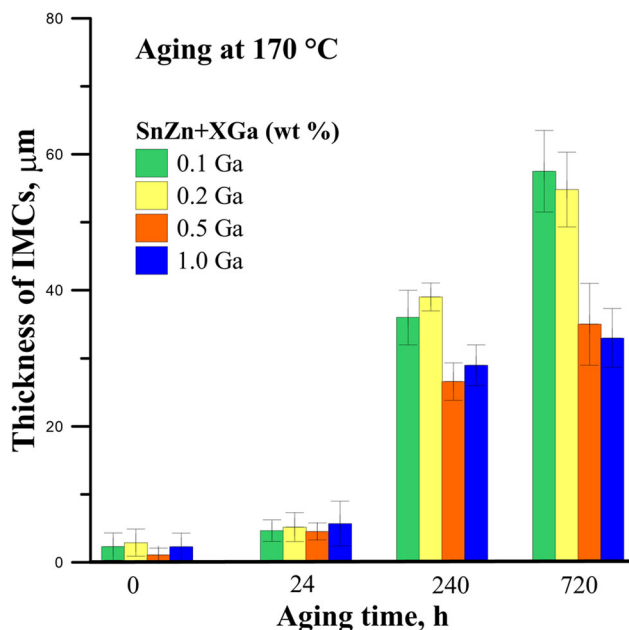
Fig. 7 Thickness of IMC layer after aging process at 170 °C for Sn-Zn-xGa alloys for different time

reacting with the Zn in the solder. Also, after 10 days of aging, the surface of the substrate in contact with the Cu_5Zn_8 layer is no longer smooth. The same character of growth of the Cu_5Zn_8 layer at the interface after the aging process was earlier observed for Sn-Zn-Bi/Cu (Ref 20) and Sn-Zn-Ag-Cu/Cu (Ref 14). A similar Zn-depleted zone was earlier observed by Ref 20 and 19. Wang et al. (Ref 19) studied aging of Sn-Zn$_{eut}$/Cu joints, which were prepared with short contact time and either very slow or rapid cooling. They explained that the initial thin intermetallic layer, when subjected to aging after rapid cooling, is not a good barrier for diffusion of Cu. But, after very slow cooling, a Cu_5Zn_8 layer formed due to slow growth achieves equilibrium, and becomes an effective barrier for the fast diffusion of Cu to the solder (Ref 19).

Figure 6, shows higher magnification micrographs of the Sn-8.9Zn-0.5Ga/Cu interface after aging treatment. The inclusions of Sn and another phase are observed from the Cu substrate side after 240 h. Based on EDS analysis results, this phase is identified as Cu_6Sn_5. It is a product of the reaction of Cu with Sn, which diffused through the Cu_5Zn_8 layer from the Zn-depleted zone. Though the Cu_5Zn_8 phase has the lowest Gibbs free energy during aging process, growth of Cu_6Sn_5 is possible because there is no "free" Zn left in the Zn-depleted zone. Therefore it is not possible for phases from the Cu-Zn system to form. With increasing aging time, bigger inclusions of Sn and greater growth of the Cu_5Zn_8 IMC layer were observed.

The thickness of the IMC layer at the Sn-8.9Zn-xGa/Cu interface, after aging at 170 °C for different times is presented in Fig. 7. After aging for 24 h, the IMC layer shows similar thickness for all alloys regardless of Ga content. When aging time is increased to 240 and 720 h, the IMC layer grows more for 0.1 and 0.2 wt.% Ga than for 0.5 and 1.0 wt.% Ga. The effect of aging time on the interfacial microstructure evolution of Sn-9Zn-0.5Ga/Cu couples was studied by Ye et al. (Ref 11). They subjected the interfaces obtained in the wetting balance test to aging at 100 °C for 100 and 1000 h. Despite the lower

temperature, their findings agree with our results, in that the thickness of the Cu_5Zn_8 layer increases and Zn in the solder is consumed by Cu diffusing from the substrate. Sn also starts to diffuse in the opposite direction, through the Cu_5Zn_8 layer, and Cu_6Sn_5 is formed on the side of the substrate. Mayappan (Ref 20) shows that the addition of Bi to Sn-Zn caused the thickness of the IMC layers to reduce after aging at 150 °C, compared to eutectic Sn-Zn. In our case, the obtained thicknesses of 35 and 33 μm for 0.5 and 1.0 (wt.%) Ga additions to Sn-Zn are similar to eutectic Sn-Zn (33 μm) (Ref 20). However, the aging treatment temperature for Sn-Zn was 20 °C lower compared to that for Sn-Zn-Ga alloys.

4. Conclusion

The addition of Ga to Sn-Zn alloys does not have a strong effect on spreadability as a function of time and temperature. The obtained results of spreading area for Sn-Zn-Ga alloys are close to the literature data (Ref 10). In the soldering process, the thickness of the Cu_5Zn_8 IMC layer increases with time and temperature. For the Sn-Zn-0.5Ga alloy, growth of Cu_5Zn_8 IMC layer is the slowest. During aging, a Zn-depleted zone is observed on the side of the solder and Cu_6Sn_5 is found on the side of the substrate after 10 days. The initial thin Cu_5Zn_8 layer is no barrier for Sn and Cu diffusion during aging.

References

1. L. Zhang, S. Xue, L. Gao, Z. Sheng, H. Ye, Z. Xiao, G. Zeng, Y. Chen, and S. Yu, Development of Sn-Zn Lead-Free Solders Bearing Alloying Elements, *J. Mater. Sci.*, 2010, **21**, p 1–15
2. S. Liu, S. Xue, P. Xue, and D. Luo, Present Status of Sn-Zn Lead-Free Solders Bearing Alloying Elements, *J. Mater. Sci.*, 2015, **26**, p 4389–4411
3. T.J. Anderson and I. Ansara, The Ga-Sn (Gallium-Tin) System, *J. Phase Equilib.*, 1992, **13**, p 181–189
4. J. Dutkiewicz, Z. Moser, L. Zabdyr, D.D. Gohil, T.G. Chart, I. Ansara, and C. Girard, The Ga-Zn (Gallium-Zinc) System, *Bull. Alloy Phase Diag.*, 1990, **11**, p 77–82
5. J.-M. Song, N.-S. Liu, and K.-L. Lin, Microstructures, Thermal and Tensile Properties of Sn-Zn-Ga Alloys, *Mater. Trans.*, 2004, **45**, p 776–782
6. F.-Y. Hung, T.-S. Lui, L.-H. Chen, and P.-H. Chen, Influence of Ga addition on Microstructure, Tensile Properties and Surface Oxide Film

Characteristics of Microelectronic Sn-9Zn-xGa Solders, *Mater. Trans.*, 2008, **49**, p 1496–1502

7. T. Gancarz, Physical, Thermal, Mechanical Properties and Microstructural Characterization of Sn-9Zn-XGa Alloys, *Metall. Mater. Trans. A*, 2016, **47A**, p 326–333

8. Y. Zhang, T. Liang, and M.A. Jusheng, Phase Diagram Calculation on Sn-Zn-Ga Solders, *J. Non-Cryst. Solids*, 2004, **336**, p 153–156

9. D. Zivkovic, L. Balanovic, D. Manasijevic, T. Holjevac Grguric, D. Cubela, and A. Mitovski, Comparative Thermodynamic Analysis and Phase Diagram Prediction of the Ga‑Sn‑Zn System, *Int. J. Mater. Res.*, 2013, **104**, p 26–34

10. W.X. Chen, S.B. Xue, and H. Wang, Wetting Properties and Interfacial Microstructures of Sn-Zn-xGa Solders on Cu Substrate, *Mater. Design*, 2010, **31**, p 2196–2200

11. H. Ye, S. Xue, J. Luo, and Y. Li, Properties and Interfacial Microstructure of Sn-Zn-Ga Solder Joint with Rare Earth Pr Addition, *Mater. Design*, 2013, **46**, p 816–823

12. P. Fima, J. Pstrus, and T. Gancarz, Wetting and Interfacial Chemistry of SnZnCu Alloys with Cu and Al Substrates, *J. Mater. Eng. Perform.*, 2014, **23**, p 1530–1535

13. T. Gancarz, P. Fima, and J. Pstruś, Thermal Expansion, Electrical Resistivity, and Spreading Area of Sn-Zn-In Alloys, *J. Mater. Eng. Perform.*, 2014, **23**, p 1524–1529

14. T. Gancarz and J. Pstrus, Formation and Growth of Intermetallic Phases at the Interface in the Cu/Sn-Zn-Ag-Cu/Cu Joints, *J. Alloy. Compd.*, 2015, **647**, p 844–856

15. C. Lee and F. Shieu, Growth of Intermetallic Compounds in the Sn-9Zn/Cu Joint, *J. Electron. Mater.*, 2006, **35**, p 1660–1664

16. R. Mayappan, R.A. Zaman, Z.Z. Abidin et al., Growth of CuZn5 and Cu5Zn8 Intermetallic Compounds in the Sn-9Zn/Cu Joint During Liquid State Aging, *Adv. Mater. Res.*, 2011, **173**, p 90–95

17. Y. Huang, S. Chen, C. Chou, and W. Gierlotka, Liquidus Projection and Thermodynamic Modeling of Sn-Zn-Cu Ternary System, *J. Alloy. Compd.*, 2009, **477**, p 283–290

18. S. Terashima and T. Sasaki, Prediction of Intermetallic Compound Formation Sequences in Pseudo Binary Diffusion Couples: Experimental Examinations for (Sn-xZn)/Cu (x = 2, 5, 10, 15, 20 and 25 mass%) by Kinetic Model with Thermodynamic Data Using MDR Diagram, *Mater. Trans.*, 2014, **55**, p 1750–1754

19. J.-Y. Wang, C.-F. Lin, and C.-M. Chen, Retarding the Cu5Zn8 Phase Fracture at the Sn-9 wt.% Zn/Cu Interface, *Scripta Mater.*, 2011, **64**, p 633–636

20. R. Mayappan and Z. Ahmad, Effect of Bi Addition on the Activation Energy for the Growth of Cu5Zn8 Intermetallic in the Sn-Zn Lead-Free Solder, *Intermetallics*, 2010, **18**, p 730–735